Experimental Demonstration of a 10 Gb/s Subcarrier Multiplexed WDM PON

Jonathan M. Buset, *Student Member, IEEE*, Ziad A. El-Sahn, *Member, IEEE*, and David V. Plant, *Fellow, IEEE*

***Abstract*— We experimentally demonstrate a 10 Gb/s bidirectional subcarrier multiplexed (SCM) wavelength-division multiplexed (WDM) passive optical network (PON). We use digital signal processing and square-root raised cosine pulse shaping techniques to generate M-ary quadrature amplitude modulation electrical signals for the downlink and uplink transmissions using simple intensity modulation and direct detection optoelectronics, and 10 GHz transceivers. The design includes spectral pre-emphasis and offset optical filtering to increase the effective bandwidth of a commercial 2.2 GHz reflective semiconductor optical amplifier based optical network unit. We realize symmetric 10 Gb/s transmission over a 20 km single feeder PON with optical line terminal launch powers from 1 to 9 dBm. We also demonstrate the ability of these SCM WDM PONs to withstand the effects of upstream impairments.**

***Index Terms*— Passive optical network (PON), reflective semiconductor optical amplifier (RSOA), subcarrier multiplexing (SCM), wavelength-division multiplexing (WDM).**

I. Introduction

CAPACITIES in access networks must evolve as consumer appetites for high bandwidth services such as streaming Internet video, video-on-demand and cloud-based storage continue to grow. Passive optical networks (PONs) using time-division multiplexing (TDM) are now standardized at 10 Gb/s of aggregate bandwidth [1], but scaling beyond this rate is expected to be technically challenging [2]. Wavelength-division multiplexed (WDM) PONs that build on existing transport network technologies are expected to provide the flexibility and capacity to meet future needs upwards of 10 Gb/s per user [3]. To be economically viable, WDM PONs should require only minimal upgrades to the existing deployed TDM PON infrastructure: They should maintain a single feeder architecture, while arrayed waveguide gratings (AWGs) will replace the passive power splitters at the remote node (RN). Colourless optical network units (ONUs) are necessary to eliminate inventory redundancy for the network operator.

Digital signal processing (DSP) is a proven effective technique for next generation transport network systems as it replaces expensive optical components with high-speed transceiver electronics [4]. There is great potential for access networks to build on these DSP techniques using lower speed electronic components to achieve significant performance increases from economical optoelectronic transceivers.

Subcarrier multiplexing (SCM) is known to be especially effective at eliminating noise due to inter-channel crosstalk and reflections in WDM PONs with downlink remodulation [5], but previous demonstrations were limited to data rates less than 10 Gb/s [6] or required high bandwidth receivers [7].

In this letter we extend the concepts proposed in our initial demonstration [8] and present the performance of a SCM WDM PON with symmetric 10 Gb/s per wavelength transmission using commodity intensity modulation (IM)/direct detection (DD) transceivers, and bidirectional transmission on the same wavelength. This DSP architecture transmits M-ary quadrature amplitude modulation (M-QAM) data signals for the uplink and downlink that are multiplexed on different subcarrier frequencies in the electrical domain [9], providing robust resistance to the inter-channel noise due to reflections and Rayleigh backscattering (RB) [10]. We use DSP spectral pre-compensation, offset optical filtering [11] and electronic equalization [12] to compensate for the bandwidth-limited reflective semiconductor optical amplifier (RSOA)-based ONU transmitter. We demonstrate symmetric operation over a wide range of optical line terminal (OLT) launch powers from 1 dBm to 9 dBm, assuming standard Reed-Solomon (RS) forward error correction (FEC) codes with 12.5% overhead.

II. DSP Enabled SCM WDM PON

A. PON Physical Architecture

Fig. 1 illustrates the single feeder architecture used in this experiment. The optical line terminal (OLT) transmitter consists of a Micram VEGA digital-to-analog converter (DAC) with 6 bit precision driving an electro-absorption modulated laser (EML) centred at 1549.41 nm. Following the EML, a booster EDFA and VOA control the launch power P_{OLT_Tx}, as measured at the circulator output. The downlink extinction ratio (ER) is set with a bias-tee to achieve a minimum bit error ratio (BER). The optical distribution network (ODN) comprises a 20.35 km feeder of standard single mode fiber (SMF-28e+), a 100 GHz AWG and a 1.5 km distribution drop fiber (DDF). At the ONU, 80% of the downstream signal is tapped off for detection by the receiver comprised of a p-i-n photoreceiver, a RF amplifier, and a real-time oscilloscope performing 8 bit precision analog-to-digital conversion (ADC). The remaining 20% of the downstream signal seeds a RSOA with peak gain from 1530 nm to 1570 nm and 2.2 GHz modulation bandwidth. The RSOA uplink transmitter is directly modulated at 4 $V_{p\text{-}p}$, biased at 80 mA, and driven by

Manuscript received April 16, 2013; revised May 28, 2013; accepted May 30, 2013. Date of publication June 6, 2013; date of current version July 9, 2013.

J. M. Buset and D. V. Plant are with the Photonic Systems Group, Department of Electrical and Computer Engineering, McGill University, Montréal H3A 2A7, Canada (e-mail: jonathan.buset@mail.mcgill.ca; david.plant@mcgill.ca).

Z. A. El-Sahn was with the Photonic Systems Group, Department of Electrical and Computer Engineering, McGill University, Montréal H3A 2A7, Canada. He is now with the Electrical Engineering Department, Alexandria University, Alexandria 21544, Egypt (e-mail: ziad.elsahn@alexu.edu.eg).

Digital Object Identifier 10.1109/LPT.2013.2266615

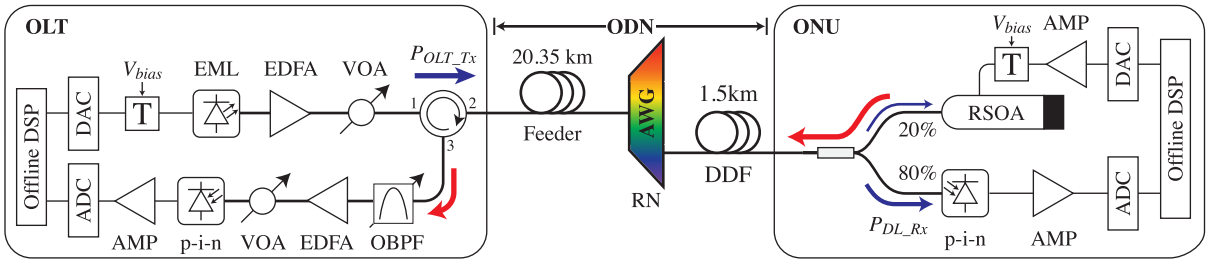

Fig. 1. Physical architecture of the proposed SCM WDM PON. The saturation input power of the RSOA is −17 dBm. The ONU coupling ratio is carefully selected to optimize the power budgets of both transmissions, maximizing the detected downlink power P_{DL_Rx} while minimizing the RB contribution of the upstream transmission by maintaining the ONU gain below the ODN losses (9.8 dB). AMP: RF amplifier, EDFA: erbium-doped fiber amplifier, EML: electro-absorption modulated laser (CyOptics E4560), OBPF: 0.30 nm optical band-pass filter (JDSU VCF050), p-i-n: 10 GHz photoreceiver (DSC-R402), RN: remote node, RSOA: reflective semiconductor optical amplifier (CIP SOA-RL-OEC-1550), T: RF bias-tee, VOA: variable optical attenuator.

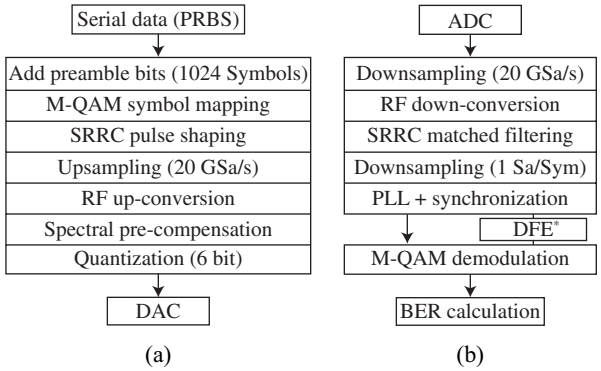

Fig. 2. Block diagrams of the (a) transmitter and (b) receiver DSP stacks used for offline processing of the downlink and uplink signals. *Note that DFE post-compensation is not performed on the received downlink signal.

a second VEGA DAC. The OLT receiver consists of a 0.30 nm tunable optical band pass filter (OBPF), a pre-amp EDFA and VOA to fix the received power at −2 dBm, along with a p-i-n photoreceiver, a RF amplifier and an ADC to capture the received signal. In addition to the DSP pre-compensation, the effective uplink bandwidth is further increased by offsetting the centre of the OBPF from the peak upstream wavelength by −0.18 nm.

B. Software Enabled DSP Transceivers

Fig. 2 outlines the general flow of the transmitter and receiver software stacks, which we use during offline processing. At the transmitters, $2^{23}-1$ and $2^{31}-1$ length pseudo-random bit sequences (PRBSs) are generated offline for the downlink and uplink, respectively. A short ∼1 kSymbol preamble is added to the beginning of each sequence. After symbol mapping (16-QAM for downlink, QPSK for uplink) the sequences are truncated to 512 kSymbol due to DAC memory limitations. A square-root raised cosine (SRRC) filter of order 128 is then applied to increase the spectral efficiency and reduce the effects of ISI. Each signal is then upsampled and multiplexed on a RF subcarrier, spanning a first null electrical bandwidth

$$B_{ch} = (1 + \alpha_{ch}) \times R_{sym}, \tag{1}$$

where α_{ch} is the roll off factor and R_{sym} is the symbol rate.

Prior to transmission, a 16th order finite impulse response (FIR) filter with 50 ps tap spacing is applied to the signal to pre-compensate for each channel's bandwidth limiting component. This flattens the power spectrum over the band of interest enabling transmission and reception of M-QAM electrical signals with low-cost optoelectronics. The DACs then drive the optical transmitters with the quantized signals.

The data captured at 40 GSa/s by the ADC receiver is downsampled, RF down-converted, and a matched SRRC filter (order 128) is applied to eliminate ISI and remove out-of-band noise. After the timing synchronization and M-QAM decision blocks, the preamble symbols are used to remove the phase-locked loop (PLL) phase ambiguity. At the OLT receiver, post-compensation is optionally performed on the uplink signal using a decision feedback equalizer (DFE) comprising 4 forward and 1 backward symbol-spaced taps. The DFE taps are initially trained using the preamble symbols and then dynamically adjusted using the least-mean square (LMS) algorithm. The signal is then demodulated for BER calculation using approximately 4×10^6 bit of binary data.

III. Experimental Results & Discussion

A. Downlink

The downlink channel consists of a 2.5 Gbaud 16-QAM signal with a SRRC roll off factor of 0.35 resulting in a spectral efficiency of 2.96 bit/s/Hz. To provide spectral separation from the uplink channel, the downlink is centred on a 7.66 GHz subcarrier. Fig. 3 presents a study of the downstream BER performance as a function of P_{OLT_Tx} with and without the aid of spectral pre-compensation.

The roll off of the p-i-n (−3 dB bandwidth ∼9.5 GHz), and to a lesser extent the EML, distorts the upper portion of the channel causing a mismatch of the SRRC filter applied at the ONU receiver and thus violates the *Nyquist pulse shaping criterion*. The resulting BER of the uncompensated downlink channel reaches an error floor near 10^{-2}. When the transciever distortion is pre-compensated for at the OLT, downlink BERs below the RS(255,223) FEC threshold of 1.1×10^{-3} [1] can be achieved for P_{OLT_Tx} greater than 0 dBm and quickly reach the calculation floor of $\sim 10^{-5}$. For $P_{OLT\_Tx} \geq 5$ dBm this results in a BER improvement of three orders of magnitude.

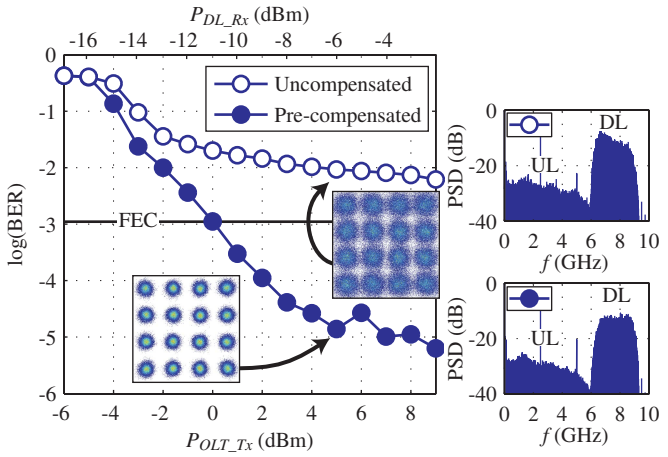

Fig. 3. BER performance of the 2.5 Gbaud 16-QAM downlink transmissions after 20 km. Constellation diagrams and electrical power spectra at $P_{OLT\_Tx} = 5$ dBm are inset as indicated. The corresponding P_{DL_Rx} at the ONU indicates a received power sensitivity of -11 dBm. We note the presence of uplink channel RB noise due to the simultaneous upstream transmission.

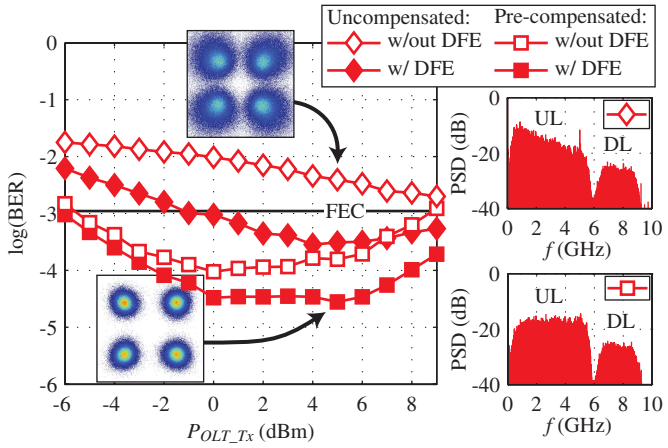

Fig. 4. BER performance of the uplink channel with and without spectral pre-compensation for the RSOA. Constellation diagrams and electrical power spectra at $P_{OLT\_Tx} = 5$ dBm are inset as indicated. The OBPF is offset by -0.18 nm resulting in an average loss of 6.6 dB, including insertion losses. We also note the presence of the residual downlink channel which was amplified and reflected by the RSOA.

B. Uplink

The uplink channel comprises a 5 Gbaud QPSK signal with a 0.15 roll off factor transmitted on a 2.97 GHz subcarrier. The smaller roll off factor gives a 1.74 bit/s/Hz spectral efficiency and allows the uplink channel to occupy only 5.75 GHz. Maintaining the uplink channel away from baseband also provides some spectral separation from the low frequency RB beat noise [13]. Fig. 4 characterizes the BER performance of the uplink transmission both with and without pre-compensation.

The uncompensated transmission cannot operate below the FEC threshold without an additional post-compensation DFE stage at the receiver. In the inset spectrum, we see that the received uplink signal has a power imbalance of nearly 10 dB over the width of the channel. Similar to nonreturn-to-zero (NRZ) modulated signals [12], the linear roll off of the RSOA enables the DFE to improve the performance and achieve BERs below the FEC threshold for $P_{OLT\_Tx} \geq 0$ dBm.

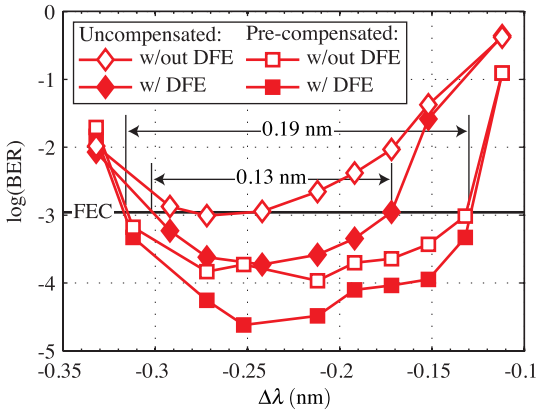

Fig. 5. The impact of offset filtering and spectral pre-compensation on the uplink BER. $\Delta\lambda = \lambda_{filter} - \lambda_{UL}$, where λ_{filter} is the filter passband centre and λ_{UL} is the uplink channel's peak wavelength. $P_{OLT\_Tx} = 5$ dBm.

Pre-compensating for the RSOA roll off flattens the uplink channel, lowers the minimum required launch power by 6 dB and sustains operation up to 9 dBm. The BER reaches an error floor near 10^{-4}, which can further be reduced to $\sim 3 \times 10^{-5}$ with a DFE. Using the uplink electrical power spectra inset in Fig. 4, we observe that the combination of DSP pre-compensation and offset optical filtering results in a *flat* received power spectrum throughout the 6 GHz channel band.

Optical filter detuning has been shown to increase the RSOA's effective bandwidth by transforming the unwanted phase modulation due to the device's transient chirp into IM [11]. Recently, this technique was demonstrated by tuning a narrow bandwidth AWG at the OLT, to simultaneously enhance the received signals and separate the WDM channels for detection [14]. Fig. 5 demonstrates the sensitivity of the uplink performance to the OBPF offset.

For the uncompensated transmission, the uplink BER only dips below the FEC threshold at -0.27 nm. As found previously for NRZ signals [11], adding a DFE at the receiver reduces the wavelength sensitivity and widens the operating region of the offset filtering to 0.13 nm ($\sim$16 GHz).

The ONU pre-compensation filter is optimized for each $\Delta\lambda$ to provide an upper bound on the system performance. In this case, the trends of the curves are the same regardless of whether or not a DFE is used. Pre-compensation reduces optical losses by achieving operation at the minimum $\Delta\lambda$ of -0.13 nm. It simultaneously widens the operating region of the offset filtering to 0.19 nm ($\sim$24 GHz) significantly lowering the system's overall sensitivity to laser wavelength drift. This improvement may be due in part to the added sensitivity resulting from pre-amplification at the OLT.

C. Upstream Impairments

There are three primary contributors to upstream impairments in bidirectional WDM PONs: Reflections, inter-channel crosstalk and RB [10]. Stimulated Brillouin scattering (SBS) also becomes a major impairment at $P_{OLT\_Tx} > 6$ dBm [15]. In this letter, the impact of static reflections is minimized by using optical connectors with oblique end facets. In wavelength re-use systems where the RSOA is seeded with

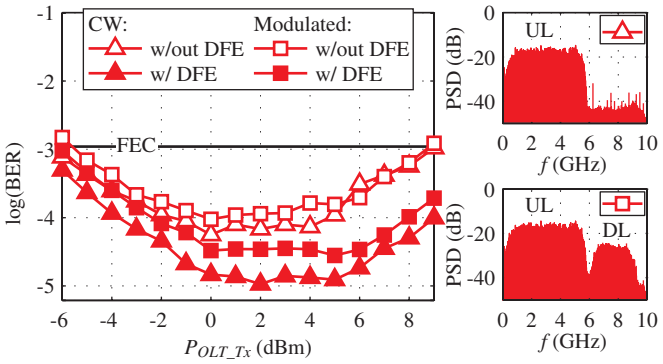

Fig. 6. Comparison of the uplink BER performance with CW and modulated downlink seed light. Electrical power spectra at $P_{OLT\_Tx} = 5$ dBm are inset as indicated. $\Delta\lambda = -0.18$ nm.

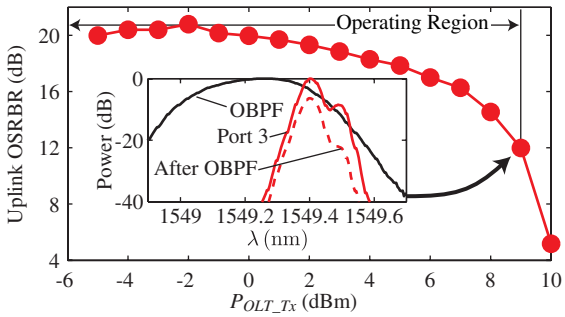

Fig. 7. Influence of backscattering on the uplink channel performance. The inset illustrates that the system's resilience to SBS is a direct result of the offset filter, as its characteristic 10 GHz frequency offset sets it further down the stop band. The OBPF profile is included for reference.

a modulated downlink signal, inter-channel crosstalk results from incomplete erasure of the downlink data and impacts the uplink transmission [16]. Fig. 6 illustrates the effect of downlink modulation on the uplink channel BER performance.

When compared to a remote continuous wave (CW) seed, there is no power penalty in terms of P_{OLT_Tx} as a result of downlink modulation, and only a 1.5–2× increase in BER. This is important in two ways: 1) here the downlink ER is *maximized* to facilitate 16-QAM signals; and 2) the residual downlink noise is still strongly present in the downlink channel band due to the high-pass filtering effect of the gain saturated RSOA. These results confirm that strong erasure of the downlink is not required for wavelength re-use in this M-QAM SCM system because the RF channels are spectrally separated and the out-of-band noise is efficiently removed in DSP at the receiver.

The impairment of RB on bidirectional PONs has been well studied [10] and Fig. 7 demonstrates its effect on the uplink optical signal-to-RB ratio (OSRBR), as measured at the port 3 output of the OLT circulator [15]. The behaviour of the OSRBR measurement corresponds well to the BER curves in Figs. 4 and 6. At launch powers ≤ 0 dBm the OSRBR remains constant ~20 dB where the BER steadily decreases with P_{OLT_Tx} indicating a power limited system. As the launch power increases further, the OSRBR slowly decreases as the RSOA's gain saturates, causing the BER curves to reach an error floor as the system becomes RB noise limited. With the onset of SBS above 6 dBm it becomes the dominant noise source on the upstream signal and increases the uplink BER. The system remains operational at 9 dBm corresponding to just 12 dB of OSRBR.

IV. Conclusion

In this letter we present a SCM WDM PON with symmetric 10 Gb/s bidirectional transmission over a single 20 km feeder. This architecture uses DSP spectral pre-compensation and offset optical filtering techniques to optimize the performance of low cost IM/DD optoelectronic transceivers. Spectrally efficient high-order M-QAM signals enable SCM in just 10 GHz of electrical bandwidth. We demonstrate operation over a wide range of launch powers from 1 dBm to 9 dBm and establish the system's resilience to upstream impairments.

References

[1] K. Tanaka, A. Agata, and Y. Horiuchi, "IEEE 802.3av 10G-EPON standardization and its research and development status," *J. Lightw. Technol.*, vol. 28, no. 4, pp. 651–661, Feb. 15, 2010.

[2] D. Breuer, *et al.*, "Requirements and solutions for next-generation access," in *Proc. ITG Symp. Photon. Netw.*, May 2011, pp. 1–8.

[3] J.-I. Kani, "Enabling technologies for future scalable and flexible WDM-PON and WDM/TDM-PON systems," *IEEE J. Sel. Topics Quantum Electron.*, vol. 16, no. 5, pp. 1290–1297, Sep. 2010.

[4] K. Roberts, D. Beckett, D. Boertjes, J. Berthold, and C. Laperle, "100G and beyond with digital coherent signal processing," *IEEE Commun. Mag.*, vol. 48, no. 7, pp. 62–69, Jul. 2010.

[5] K. Y. Cho, A. Murakami, Y. Lee, A. Agata, Y. Takushima, and Y. C. Chung, "Demonstration of RSOA-based WDM PON operating at symmetric rate of 1.25 Gb/s with high reflection tolerance," in *Proc. OFC/NFOEC*, Feb. 2008, pp. 1–3.

[6] J. M. Buset, Z. A. El-Sahn, and D. V. Plant, "Bandwidth efficient bidirectional 5 Gb/s overlapped-SCM WDM PON with electronic equalization and forward-error correction," *Opt. Express*, vol. 20, no. 13, pp. 14428–14436, Jun. 2012.

[7] Z. Al-Qazwini and H. Kim, "Symmetric 10-Gb/s WDM-PON using directly modulated lasers for downlink and RSOAs for uplink," *J. Lightw. Technol.*, vol. 30, no. 12, pp. 1891–1899, Jun. 15, 2012.

[8] J. M. Buset, Z. A. El-Sahn, and D. V. Plant, "Demonstration of a symmetric 10 Gb/s QPSK subcarrier multiplexed WDM PON with IM/DD transceivers and a bandwidth-limited RSOA," in *Proc. OFC/NFOEC*, Mar. 2013, pp. 1–3.

[9] J.-M. Kang and S.-K. Han, "A novel hybrid WDM/SCM-PON sharing wavelength for up- and down-link using reflective semiconductor optical amplifier," *IEEE Photon. Technol. Lett.*, vol. 18, no. 3, pp. 502–504, Feb. 1, 2006.

[10] C. Arellano, K. Langer, and J. Prat, "Reflections and multiple Rayleigh backscattering in WDM single-fiber loopback access networks," *J. Lightw. Technol.*, vol. 27, no. 1, pp. 12–18, Jan. 1, 2009.

[11] I. Papagiannakis, *et al.*, "Investigation of 10-Gb/s RSOA-based upstream transmission in WDM-PONs utilizing optical filtering and electronic equalization," *IEEE Photon. Technol. Lett.*, vol. 20, no. 24, pp. 2168–2170, Dec. 15, 2008.

[12] K. Y. Cho, Y. Takushima, and Y. C. Chung, "10-Gb/s operation of RSOA for WDM PON," *IEEE Photon. Technol. Lett.*, vol. 20, no. 18, pp. 1533–1535, Sep. 15, 2008.

[13] A. Chiuchiarelli, *et al.*, "Enhancing resilience to Rayleigh crosstalk by means of line coding and electrical filtering," *IEEE Photon. Technol. Lett.*, vol. 22, no. 2, pp. 85–87, Jan. 15, 2010.

[14] M. Presi, *et al.*, "Enhanced 10 Gb/s operations of directly modulated reflective semiconductor optical amplifiers without electronic equalization," *Opt. Express*, vol. 20, no. 26, pp. B507–B512, Dec. 2012.

[15] J. L. Wei, E. Hugues-Salas, R. P. Giddings, X. Q. Jin, X. Zheng, S. Mansoor, and J. M. Tang, "Wavelength reused bidirectional transmission of adaptively modulated optical OFDM signals in WDM-PONs incorporating SOA and RSOA intensity modulators," *Opt. Express*, vol. 18, no. 10, pp. 9791–9808, Apr. 2010.

[16] W. Lee, *et al.*, "Bidirectional WDM-PON based on gain-saturated reflective semiconductor optical amplifiers," *IEEE Photon. Technol. Lett.*, vol. 17, no. 11, pp. 2460–2462, Nov. 2005.